Title

Hyperconnectivity of Two Separate Long-Range Cholinergic Systems Contributes to the Reorganization of the Brain Functional Connectivity during Nicotine Withdrawal in Male Mice

Journal

eNeuro, 10(6)

ISSN

2373-2822

Authors

Carrette, Lieselot LG
Kimbrough, Adam
Davoudian, Pasha A
et al.

Publication Date

2023-06-01

DOI

10.1523/eneuro.0019-23.2023

Peer reviewed

eNeuro

Research Article: New Research

Disorders of the Nervous System

Hyperconnectivity of Two Separate Long-Range Cholinergic Systems Contributes to the Reorganization of the Brain Functional Connectivity during Nicotine Withdrawal in Male Mice

Lieselot L. G. Carrette,[1] Adam Kimbrough,[1] Pasha A. Davoudian,[2,3] Alex C. Kwan,[4] Andres Collazo,[5] and Olivier George[1]

https://doi.org/10.1523/ENEURO.0019-23.2023

[1]Department of Psychiatry, UC San Diego, California 92093, [2]Medical Scientist Training Program, Yale University School of Medicine, New Haven, Connecticut 06511, [3]Interdepartmental Neuroscience Program, Yale University School of Medicine, New Haven, Connecticut 06511, [4]Meinig School of Biomedical Engineering, Cornell University, Ithaca, New York 14853, and [5]Beckman Institute, California Institute of Technology, Pasadena, California 91125

Visual Abstract

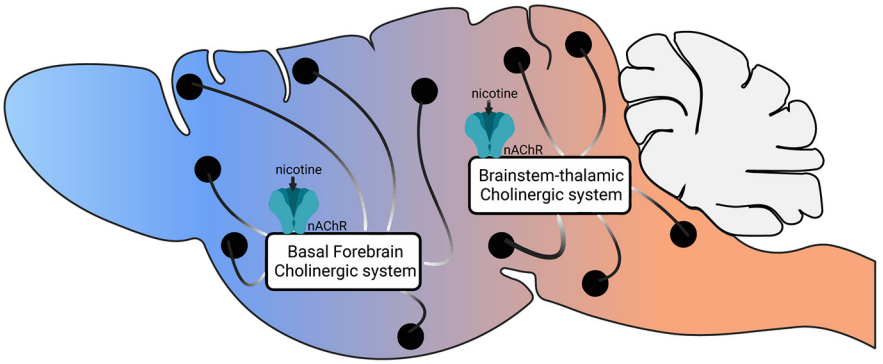

Chronic nicotine results in dependence with withdrawal symptoms on discontinuation of use, through desensitization of nicotinic acetylcholine receptors and altered cholinergic neurotransmission. Nicotine withdrawal is associated with increased whole-brain functional connectivity and decreased network modularity; however, the role of cholinergic neurons in those changes is unknown. To identify the contribution of nicotinic receptors and cholinergic regions to changes in the functional network, we analyzed the contribution of the main cholinergic regions to brain-wide activation of the immediate early-gene Fos during withdrawal in male mice and

Significance Statement

Discontinuation of nicotine use in dependent users is associated with increased whole-brain activation and functional connectivity and leads to withdrawal symptoms. Here we investigated the contribution of the nicotinic cholinergic receptors and main cholinergic projecting brain areas in the whole-brain changes associated with withdrawal. This not only allowed us to visualize and confirm the previously described duality of the cholinergic brain system using this novel methodology, but also identify nicotinic receptors together with 1751 other genes that contribute to, and could thus be targets for treatments against, nicotine withdrawal and dependence.

correlated these changes with the expression of nicotinic receptor mRNA throughout the brain. We show that the main functional connectivity modules included the main long-range cholinergic regions, which were highly synchronized with the rest of the brain. However, despite this hyperconnectivity, they were organized into two anticorrelated networks that were separated into basal forebrain-projecting and brainstem-thalamic-projecting cholinergic regions, validating a long-standing hypothesis of the organization of the brain cholinergic systems. Moreover, baseline (without nicotine) expression of *Chrna2*, *Chrna3*, *Chrna10*, and *Chrnd* mRNA of each brain region correlated with withdrawal-induced changes in Fos expression. Finally, by mining the Allen Brain mRNA expression database, we were able to identify 1755 gene candidates and three pathways (Sox2-Oct4-Nanog, JAK-STAT, and MeCP2-GABA) that may contribute to nicotine withdrawal-induced Fos expression. These results identify the dual contribution of the basal forebrain and brainstem-thalamic cholinergic systems to whole-brain functional connectivity during withdrawal; and identify nicotinic receptors and novel cellular pathways that may be critical for the transition to nicotine dependence.

Key words: addiction; Fos reactivity; single-cell whole-brain imaging; stimulant

Introduction

Chronic nicotine use causes adaptive changes throughout the brain that lead to drug dependence (Markou, 2008; Martin-Soelch, 2013; Fowler et al., 2020), the emergence of a withdrawal state following cessation, and long-lasting somatic and motivational symptoms (Le Foll and Goldberg, 2009) that contribute to relapse (Allen et al., 2008; Zhou et al., 2009). Brain states, like dependence and withdrawal, have been described through patterns of synchronous neural firing (Brown, 2006). Changes in the patterns of neuronal coreactivity, also called the functional connectome, can be observed in humans and rodents during withdrawal from nicotine (Hobkirk et al., 2018; Cheng et al., 2019; Kimbrough et al., 2021). Whole-brain imaging with single-cell resolution using light-sheet microscopy on cleared brains (Renier et al., 2014, 2016; Ueda et al., 2020) has made the study of brain-wide functional networks at single-cell resolution possible by looking at the expression of the immediate-early gene Fos (Wheeler et al., 2013; Vetere et al., 2017; Kimbrough et al., 2020; 2021; Smith et al., 2021; Roland et al., 2022), a marker of neuronal reactivity, which integrates neuronal activation during a period of 1–2 h, an ideal temporal window to characterize nicotine withdrawal. Using this approach, we have found that mice in withdrawal exhibit a pronounced increase in coactivation patterns throughout the brain (Kimbrough et al., 2020, 2021). A healthy control brain is modularly organized in several small, correlated clusters or modules consisting of brain regions that are functionally related. The withdrawal-induced increase in correlation between brain regions causes more regions to cluster together with a significant decrease in whole-brain modularity. Increased functional connectivity throughout the network also results in a reduction of brain regions identified as hubs. Hub regions are regions with the highest intramodular and intermodular connectivity as measured using graph theory (participation coefficient, within-module degree). These hub regions are hypothesized to be the biggest drivers of neuronal activity within the network. For instance, during nicotine withdrawal, the main hub regions shift from cortical (e.g., sensory, motor) to subcortical (e.g., amygdalar, thalamic, hypothalamic, and midbrain) regions (Kimbrough et al., 2020, 2021). However, the role of cholinergic neurons and cholinergic receptors in the whole-brain functional hyperconnectivity observed during withdrawal is unknown.

Desensitization and upregulation of nicotinic acetylcholine receptors (nAChRs) (Benwell et al., 1988; Balfour and Fagerström, 1996; Dani and Heinemann, 1996; Fowler et al., 2020) contributes to the emergence of nicotine withdrawal symptoms by altering cholinergic neurotransmission in brain regions critical to sensory processing (Gil and Metherate, 2019), attention (Hahn, 2015), emotion, and motivation (Leslie et al., 2013). nAChRs form pentameric structures assembled from a family of subunits composed of α_2–α_{10} and β_2–β_4. α_4 and β_2 are the most prevalent, but all subunits are expressed throughout the brain. A large number of brain regions (40+) have cholinergic neurons, characterized by the expression of choline acetyltransferase (ChAT); however, most of them are interneurons, and only eight brain regions have long-range projecting cholinergic neurons (Mesulam et al., 1983). The long-range cholinergic regions include Ch1 [medial septal nucleus (MS)], Ch2 [vertical nucleus of the diagonal band (NDB)], Ch3 [horizontal limb of the NDB], Ch4 [nucleus basalis of Meynert that consists of the magnocellular nucleus (MA) and substantia innominata (SI)], Ch5 [pedunculopontine

Received December 19, 2022; accepted April 25, 2023; First published June 9, 2023.

The authors declare no competing financial interests.

Author contributions: L.L.G.C. and O.G. designed research; L.L.G.C. and A.C. performed research; A.K., P.D., and A.C.K. contributed unpublished reagents/analytic tools; L.L.G.C. and O.G. analyzed data; L.L.G.C. and O.G. wrote the paper.

Support was received from the Preclinical Addiction Research Consortium. This work was supported by National Institute on Drug Abuse Grant 1R21-DA-057694; Tobacco-Related Disease Research Program Grants 27IR0047 and 32IR5384 to O.G.; and Innovation Award 3901 from the International Rett Syndrome Foundation to L.L.G.C. National Institute of Mental Health Grant R01MH128217 to A.C.K.; National Institute on Drug Abuse Grant F30DA059437 to P.A.D. Publication fees were contributed by the UC San Diego library.

A. Kimbrough's present address: Department of Basic Medical Sciences, College of Veterinary Medicine, Purdue University, West Lafayette, IN 47906.

Correspondence should be addressed to Lieselot L. G. Carrette at lcarrette@health.ucsd.edu or Olivier George at olgeorge@health.ucsd.edu.

https://doi.org/10.1523/ENEURO.0019-23.2023

nucleus (PPN)], Ch6 [laterodorsal tegmental nucleus], Ch7 [medial habenula (MH)], and Ch8 [parabigeminal nucleus] (Mesulam et al., 1983; Woolf, 1991). We hypothesized that, following chronic nicotine administration, most cholinergic regions that are rich in nicotinic receptors would have a synchronized correlated activity due in part to the brain-wide upregulation of nicotinic receptors (Govind et al., 2009; Fowler et al., 2020) and the increase in cholinergic transmission during nicotine withdrawal (Carcoba et al., 2014). The increased correlation would lead to larger modules and decreased modularity. Furthermore, since cholinergic receptor signaling is critical for nicotine-induced Fos activation (Pang et al., 2016; Simmons et al., 2016), a subhypothesis was that the regional expression level of cholinergic-related genes would be correlated to regional differential Fos expression under withdrawal in nicotine-dependent animals.

To test these hypotheses, we reanalyzed the previously published whole-brain nicotine withdrawal network (Kimbrough et al., 2021) focusing on the cholinergic regions using hierarchical clustering and graph theory analysis, and investigated the relationship between baseline gene expression levels and Fos reactivity using the whole-brain *in situ* Allen Brain expression database, which contains the regional whole-brain expression of 19,413 genes in the mouse genome (Lein et al., 2007; Davoudian et al., 2023). Contrary to our hypothesis, we found that during nicotine withdrawal, the cholinergic regions did not cluster together in a single module but were instead represented in each of the main modules and organized into two anti-correlated networks that were separated into basal forebrain projecting and brainstem-thalamic-projecting cholinergic regions. Moreover, while mRNA expression of a few nicotinic receptors correlated with Fos activation, we identified a list of >1000 candidate genes and 3 intracellular pathways that may contribute to the reorganization of the whole-brain functional connectome during nicotine withdrawal.

Materials and Methods

This report includes a reanalysis of a previously acquired and published dataset (Kimbrough et al., 2021) consisting of Fos counts per brain region (175; Extended Data Table 1-1) for two groups of male C57BL/6J mice (60 d old at the start of the experiment), 8 h after removal from minipumps (model 1002, Alzet) that were implanted in the lower back to deliver nicotine ($N = 5$, 24 mg/kg/d) or saline ($N = 4$) for 7 d. This dose was chosen based on previous studies that indicated rewarding effects during use, resulting in withdrawal-like symptoms after the cessation of chronic use (Johnson et al., 2008; Stoker et al., 2012). All brains ($N = 9$, 5 nicotine plus 4 saline) were harvested following perfusion (PBS, followed by 4% formaldehyde), postfixed overnight, immunolabeled for Fos (primary: 1:2000; catalog #226003; Synaptic Systems; and secondary: 1:500; catalog #A31573, Thermo Fisher Scientific; donkey anti-rabbit Alexa Fluor 647), cleared according to the iDISCO+ protocol, imaged using light-sheet microscopy (effective magnification, 1.6×; resolution, 4 × 4 μm; step size, 3 μm; Ultramicroscope II, LaVision BioTec), and analyzed using the ClearMap package (Renier et al., 2016). Three brain regions with low-to-no Fos counts were excluded based on quality control of the original data: the dorsal premammilary nucleus, parabigeminal nucleus, and suprachiasmatic nucleus. These experiments had been conducted in strict adherence to the National Institutes of Health *Guide for the Care and Use of Laboratory Animals*, and approved by The Scripps Research Institute Institutional Animal Care and Use Committee and by the Institutional Animal Care and Use Committee of the University of California. No new experimental procedures were performed for this article. The data were processed similarly as previously published (Kimbrough et al., 2020, 2021) using GraphPad Prism and R (code is available online at https://github.com/George-LabX), as described in more detail below.

Functional connectome construction

The Fos counts per region obtained from the published dataset, were all increased by 1 and normalized to a log10 value to reduce variability, before calculating Pearson correlations between regions. The matrix was then hierarchically clustered, based on the Euclidean distances calculated from the correlations. Modules were obtained by cutting the clustering dendrogram at half-height.

Average correlation calculations

Average R values were calculated for each treatment (saline or nicotine) within the basal forebrain cholinergic regions ($n = 3$, excluding self-correlations), within the brainstem-thalamic cholinergic regions ($n = 6$, excluding self-correlations), and between both cholinergic subgroups ($n = 12$). Average R values were also calculated per treatment for the interaction of all cholinergic regions with the major anatomic groups in the brain. Two-way ANOVA was then performed to examine the effect of treatment condition on the average R value for each comparison.

Network analysis

Networks were analyzed for centrality (degree or betweenness) with the R package iGraph. Participation coefficients were obtained using a customized version of the bctpy Python package (https://github.com/aestrivex/bctpy), derived from the MATLAB implementation of Brain Connectivity Toolbox (Rubinov and Sporns, 2010).

Analysis of expression data

Structure and gene expression data were extracted from the In Situ Hybridization gene expression database and Allen Brain Atlas (Lein et al., 2007) in Python, as published and described before [AllenSDK (https://doi.org/10.5281/zenodo.3951756); Fulcher and Fornito, 2016; Fulcher et al., 2019; Davoudian et al., 2023] and intersected with the 175 brain regions from the Fos dataset. The expression density of all nicotinic cholinergic receptors in the gene expression atlas was averaged across the experimental sets following centering and scaling per experiment. Next, the correlation of the baseline expression level (percentage of pixels) for every gene in every

experiment was correlated with the Fos expression change in withdrawal compared with control (log-fold change) per brain region for every gene. The frontal pole cerebral cortex was excluded as an outlier.

Reactome analysis

The gene set was analyzed using the Reactome pathway database on https://reactome.org/ by inserting the gene set, projected to human, and analyze without interactors (Joshi-Tope et al., 2005).

Statistical analysis

Statistical analysis was performed as indicated in GraphPad Prism software or in R Studio. For comparison of the brain states, we used two-way ANOVA with Tukey's corrected *post hoc* test[a,b] in Prism or with Mann–Whitney *U* test[c–e] in R with $p < 0.05$ (Table 1, statistics). For the gene analysis, the significance of the Pearson correlations was evaluated by calculating a *p*-value with the Pearson correlation test in R. We then used the Benjamini–Hochberg (BH) procedure to correct for multiple hypothesis testing and control the false discovery rate (FDR) at a 5% level. This method ensures that, on average, no more than 5% of the statistically significant results are expected to be false positives. By adjusting the raw *p*-values using the BH procedure, we obtained *q*-values for each test. A hypothesis test was considered statistically significant if its *q*-value was less than or equal to the predetermined FDR threshold of 0.05. This approach strikes a balance between controlling the risk of false positives and maintaining adequate statistical power, making it suitable for our analysis involving multiple comparisons.

Data visualization

Graphs were constructed using the R package ggplot2 included in the tidyverse package or the ggpubr package for barplots. Heatmaps were constructed using the R packages gplots and ComplexHeatmap. Networks were visualized by plotting in the R package igraph or using Gephi software. Pathway illustrations were created with BioRender (https://www.biorender.com/). Figures were combined and edited with Adobe Illustrator.

Data availability

The code described in the article is freely available online at https://github.com/George-LabX. Additional code and data for analyzing the whole-brain expression data are available from https://alexkwanlab.org/data/. The results were obtained by running the code in R Studio on a MacBook Pro.

Results

Cholinergic groups are distributed throughout the nicotine withdrawal network

Using the methods summarized in Figure 1*A*, the nicotine and saline control functional connectomes were obtained. Immunolabeling of immediate-early gene expression like c-*fos* captured the neuronal reactivity over a period of 1–2 h during nicotine withdrawal. Automated registration onto an anatomic reference atlas using the ClearMap pipeline (Renier et al., 2016) then allowed for unbiased quantification of neuronal activation throughout the brain. Finally, based on synchronous reactivity between functionally connected brain regions, correlation analysis of the Fos counts allowed calculation of functional distances (Fig. 1*B*,*C*, Extended Data Fig. 1-1) and construction of a whole-brain functional network that can be further analyzed using graph theory (Fig. 1*D*,*E*, thresholded for Pearson correlation > 0.75, Extended Data Figs. 1-2, 1-3). The nicotine withdrawal network consisted of 175 brain regions (nodes) with 4738 functional connections (edges), which was a 50% increase from the saline control that had 3019 functional connections. Hierarchical clustering of the correlation matrices with division of the dendrogram at half-height revealed nine modules, which was a clear decrease from the 13 modules in the control network. The five main nicotine modules included both cortical and subcortical regions, and were named based on the regions with the most significant within-module influence based on the within-module degree *z* score, which measures the intramodule connectivity or relative importance of a region within its own module (Kimbrough et al., 2021). The long-projection cholinergic groups did not cluster together in a single module as originally hypothesized, rather they were spread between the modules. All five main modules contained at least one of the eight main long-projection cholinergic groups (Ch1–8; Fig. 1*D*, circled in red). The largest cortico-mid-hindbrain module contains cholinergic group 5 (PPN). Next, the cortico-hypothalamic module contains cholinergic group 4 (MA). The intermediate cortico-hypothalamic module contains cholinergic group 1 (MS). The smaller orbitofrontal-extended amygdalar module contains cholinergic groups 2 and 3 (NDB), cholinergic group 4 (SI), and the midbrain-thalamo-habenular module cholinergic group 7 (MH) and lateral habenula (LH). The smallest modules did not have any cholinergic regions. Note that cholinergic groups 6 and 8 were omitted as they were too posterior for the imaging.

Table 1: Statistical table

	Data structure (Shapiro–Wilk test)	Type of test	Power (95% CI between saline and nicotine mean)
a	Normal	Two-way ANOVA	−0.88 to −0.14
b	Normal	Two-way ANOVA	−0.40 to −0.27
c	Non-normal	Mann–Whitney *U* test	36.00–50.00
d	Non-normal	Mann–Whitney *U* test	−63.03 to −27.80
e	Non-normal	Mann–Whitney *U* test	−0.20 to −0.11

Increased interaction of the long-range cholinergic groups throughout the brain in two subsystems

To investigate the role of the cholinergic regions in the organization of the whole-brain network, we first tested whether the long-range cholinergic groups (Fig. 2*A*) were significantly correlated with each other (Fig. 2*B*). The correlation heatmap focusing on these regions showed the emergence of two anticorrelated cholinergic subsystems during nicotine withdrawal; one in the basal forebrain

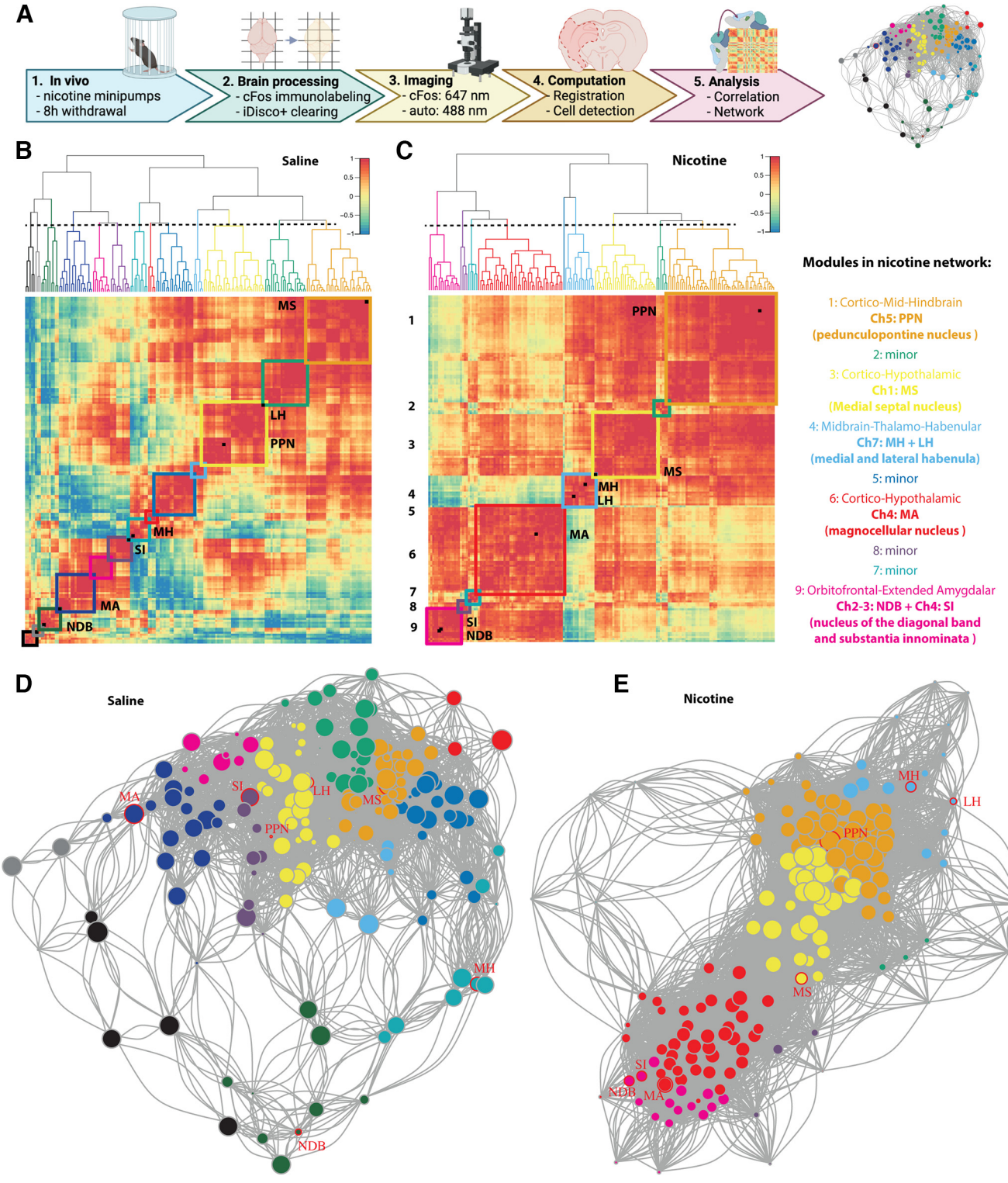

Figure 1. Functional network of nicotine withdrawal in mice. ***A***, Experimental timeline for obtaining the nicotine withdrawal functional connectome: mice were implanted subcutaneously with osmotic minipumps that delivered nicotine for 1 week, 8 h after removal brains were harvested using perfusion (1); the brains were immunolabeled for Fos and cleared using the iDISCO+ protocol (2); next, the brains were imaged using light-sheet imaging at 647 nm for Fos and 488 nm for autofluorescence (3); images were automatically registered to the Allen Brain Atlas, and active cells counted per brain region using ClearMap (4); and the Fos cell counts of each region were correlated per group to obtain distances between the regions to create a network of the brain regions, which could be further analyzed (5). ***B***, ***C***, Hierarchically clustered correlation heatmaps of the resting-state functional connectome under control conditions (saline; ***B***) or nicotine withdrawal (***C***), with 13 and 9 modules, respectively, depicted with colored squares and cholinergic regions labeled as black squares on the diagonal. The order of the brain regions in the heatmaps is available in Extended Data

continued

Figure 1-1. ***D***, ***E***, Network graph for saline (***D***) and nicotine withdrawal (***E***) with indication of cholinergic long-range regions (red circles). The node colors represent the different modules and the node size represents the degree (number of connections). A larger image of the network with labeled nodes is available in Extended Data Figures 1-1 and 1-2.

consisting of MA, NDB, and SI, and one in the brainstem-thalamic area consisting of PPN, MH, and LH, with the MS in between. Under control conditions (saline), there was no such organization. The average correlation between the cholinergic regions within the basal forebrain or within the brainstem-thalamic network was significantly higher in the nicotine group compared with the saline group (two-way ANOVA: $F_{(1,36)} = 7.85$, $p = 0.008$), with a significant difference between regions (two-way ANOVA: $F_{(2,36)} = 4.62$, $p = 0.016$), and a significant interaction (two-way ANOVA: $F_{(2,36)} = 3.36$, $p = 0.046$; Fig. 2*C*)[a]. *Post hoc* analysis confirmed that under nicotine withdrawal the average correlation within the subgroups was significantly higher than their interaction ($p < 0.04$).

We then looked at how these long-range cholinergic groups correlated with the different anatomic groups throughout the brain using hierarchical clustering within the main anatomic structures (cortical plate, cortical subplate, striatum, pallidum, thalamus, hypothalamus, midbrain, hindbrain, or cerebellum; Fig. 2*D*,*E*). There was a significant increase in correlation throughout the brain in the nicotine group compared with the saline group (two-way ANOVA: $F_{(1,2082)} = 100.7$, $p < 0.0001$), without significant difference between regions (two-way ANOVA: $F_{(8,2082)} = 1.32$, $p = 0.23$), but with significant interaction (two-way ANOVA: $F_{(8,2082)} = 3.21$, $p = 0.0012$)[b]. In line with the overall increase in correlation, the *post hoc* test showed an increase in the correlation of the cholinergic groups with the cortical plate ($p < 0.0001$), striatum ($p < 0.0001$), thalamus ($p = 0.0035$), and hypothalamus ($p < 0.0001$).

Finally, we looked at the interaction of the long-range cholinergic regions with brain regions that have been shown to be critical to nicotine addiction and nicotine withdrawal, including the anterior cingulate area (ACA; Hong et al., 2009; Wang et al., 2019; Abulseoud et al., 2020), infralimbic area (ILA; George and Koob, 2010; Huang et al., 2015; Kutlu et al., 2016), prelimbic area (PL; George and Koob, 2010; Semenova et al., 2018), dorsal peduncular area (DP; George and Koob, 2010), caudoputamen (CP; Muskens et al., 2012; Huang et al., 2015), nucleus accumbens (ACB; Rada et al., 2001; Schmidt et al., 2001; Huang et al., 2015), bed nucleus of the stria terminalis (BST; Reisiger et al., 2014; Qi et al., 2016), basolateral amygdala (BLA; Bergstrom et al., 2010; Sharp, 2019), central amygdala (CEA; Baiamonte et al., 2014; Huang et al., 2015; Funk et al., 2016), ventral tegmental area (VTA; Grieder et al., 2014; Huang et al., 2015; Wills and Kenny, 2021), and interpeduncular nucleus (IPN; Molas et al., 2017; Wills and Kenny, 2021; Klenowski et al., 2022). Here too, the minimal networks showed an overall increased functional connectivity during nicotine withdrawal, particularly among the cortex, subcortical regions, and key cholinergic regions including cholinergic groups 2, 3, 4, and 7 (PPN, MH, LH, SI, MA, and NDB), which were separated in basal forebrain and brainstem-thalamic groups (Fig. 2*F*).

Non-long-range cholinergic regions function as connector hubs in the nicotine network

To better understand the role of the cholinergic groups within the whole-brain network and to validate their role as hub regions or identify others, we calculated the network centrality measures: degree (number of connections a region has) and betweenness (number of shortest paths between two regions that go through a region). Nicotine withdrawal significantly increased the average degree ($p < 2.2e\text{-}16$[c]; Fig. 3*A*) and decreased the average betweenness of the network ($p = 2.0e\text{-}08$[d]; Fig. 3*B*). Regions that were in the top 20 of both degree and betweenness were considered hub regions (Wheeler et al., 2013). For the saline network, two hubs with both high degree and betweenness were identified: the hypothalamic parastrial area (PS) and the midbrain cuneiform nucleus (CUN). For the nicotine network, the following four hubs with those criteria were identified: the fundus of the striatum (FS), paraventricular hypothalamic nucleus (PVH), gustatory areas (GUs), and posterolateral visual areas (VISpls). The fundus of the striatum and caudoputamen stood out for having significantly higher betweenness scores than other regions, thus having a central role in the network involving shortest paths during nicotine withdrawal.

Because the networks are modular, an important role of hub regions is to act as connectors between modules, which is captured through a high participation coefficient that measures the intermodule connectivity or the extent to which a region connects to multiple other modules. Regions with a high participation coefficient were therefore also considered as hubs. Nicotine withdrawal significantly decreased the participation coefficient ($p = 3.5e\text{-}9$[e]; Fig. 3*C*). The cholinergic group 1 MS had the highest participation coefficient of the network and thus functions as a top connector between the network modules. The fundus of the striatum and caudoputamen hubs also scored high for this measure. The central role of these regions in the network is confirmed by looking at their correlation with all brain regions (Fig. 3*D*), which showed strongly increased correlation during nicotine withdrawal.

Identification of novel gene targets that correlates with brain-wide Fos activation

To examine the contribution of the regional expression level of cholinergic-related genes like the nAChRs to the organization of the functional connectome, the basal expression level of *Chrna1-10*, *Chrnb1-3*, *Chrnd*, and *ChAT* throughout the brain was extracted from the *in situ* Allen Brain database (Lein et al., 2007) and examined. While *Chrna1*, *Chrnb1*, and *Chrnd* are generally considered muscle-type subunits, expression in the brain has

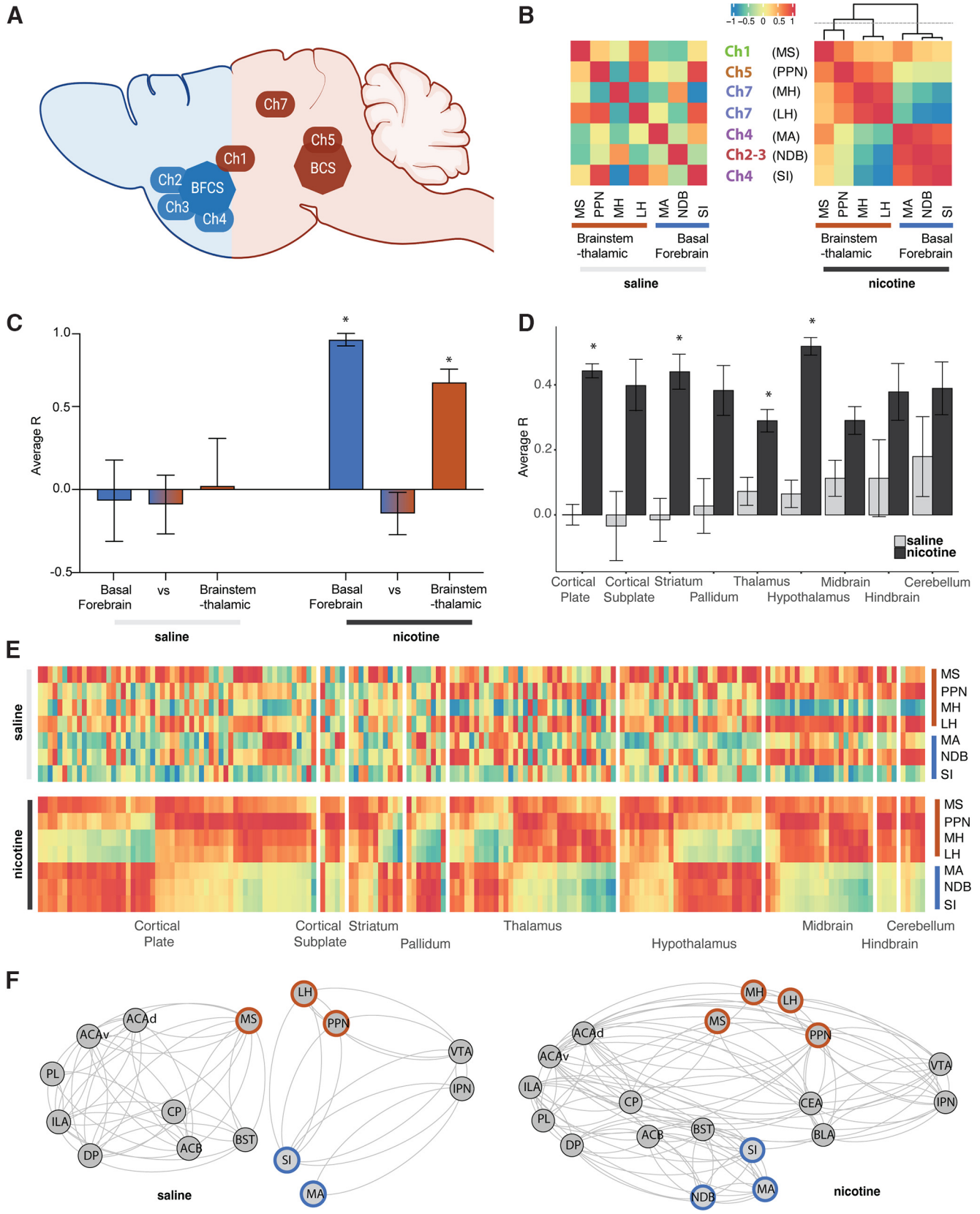

Figure 2. Interactions among the long-range cholinergic groups and with the whole-brain for saline and nicotine. ***A***, Brain schematic showing the localization and circuitry of the long-range cholinergic groups divided in basal forebrain cholinergic system (BFCS; blue) and brainstem-thalamic cholinergic system (BCS; brown), adapted from George et al. (2006). ***B***, Heatmap representation of

continued

the correlation of cholinergic long-range groups. ***C***, Average correlation (*R*) between the cholinergic long-range groups within the basal forebrain cholinergic system (blue), brainstem-thalamic cholinergic system (brown), or between ($^*p < 0.05$)[a]. ***D***, Average correlation (*R*) of cholinergic long-range groups with the rest of the brain organized into anatomic groups ($^*p < 0.05$)[b]. ***E***, Heatmap representation of ***D*** with the correlation to all individual regions in the brain (Extended Data Fig. 2-1, order of the regions). ***F***, Integration of the long-range cholinergic groups in representative minimal addiction networks.

been observed (Aishah et al., 2017). No clear pattern could be observed differentiating expression in the different modules of the functional connectome (Fig. 4*A*, left; expression within the long-range cholinergic groups is highlighted on the right). When organizing the brain regions in anatomic order on the other hand, expression patterns could be observed with *Chrna4* and *Chrnab2* being expressed mostly in the thalamus; *Chrna3*, *Chrna6*, and *Chrnb3* mostly in the midbrain; and *Chrna1*, *Chrna2*, *Chrna7*, *Chrna9*, *Chrna10*, *Chrnb1*, and *Chrnd* mostly in the cortical plate (Fig. 4*A*, middle).

Next, we wanted to compare the contribution of these cholinergic-related genes to the changes in whole-brain Fos activation and compare it with the other 19,413 genes of which the *in situ* Allen Brain database contains the region-specific gene expression (Lein et al., 2007). For every gene, we looked at the correlation between the baseline gene expression level (percentage of pixels) and the Fos expression change in nicotine withdrawal versus saline control (log-fold change) for every region (Davoudian et al., 2023; Fig. 4*B*). Significance was obtained for genes with a correlation coefficient higher than |0.23| (false discovery rate, <5%; Fig. 4*C*), which included *Chrna2*, *Chrna3*, *Chrna10* (Fig. 4*D*), and *Chrnd*. The expression of the other cholinergic-related genes did not significantly correlate with the increased induction of Fos expression during nicotine withdrawal. However, we identified 1755 genes that were significantly correlated with Fos expression during withdrawal (false discovery rate, < 5%; Extended Data Table 4-1).

To investigate the obtained gene list, it was inserted into Reactome, the free, open-source, curated, and peer-reviewed pathway database (Joshi-Tope et al., 2005), which returned the following three top hits: (1) octamer-binding transcription factor 4 (OCT4), sex-determining region Y-box 2 (SOX2), and nanog homeobox (NANOG) activate genes related to proliferation ($p = 5.12\text{e-}3$); (2) gene and protein expression by janus kinase (JAK), signal transducer and activator of transcription (STAT) signaling after Interleukin-12 stimulation

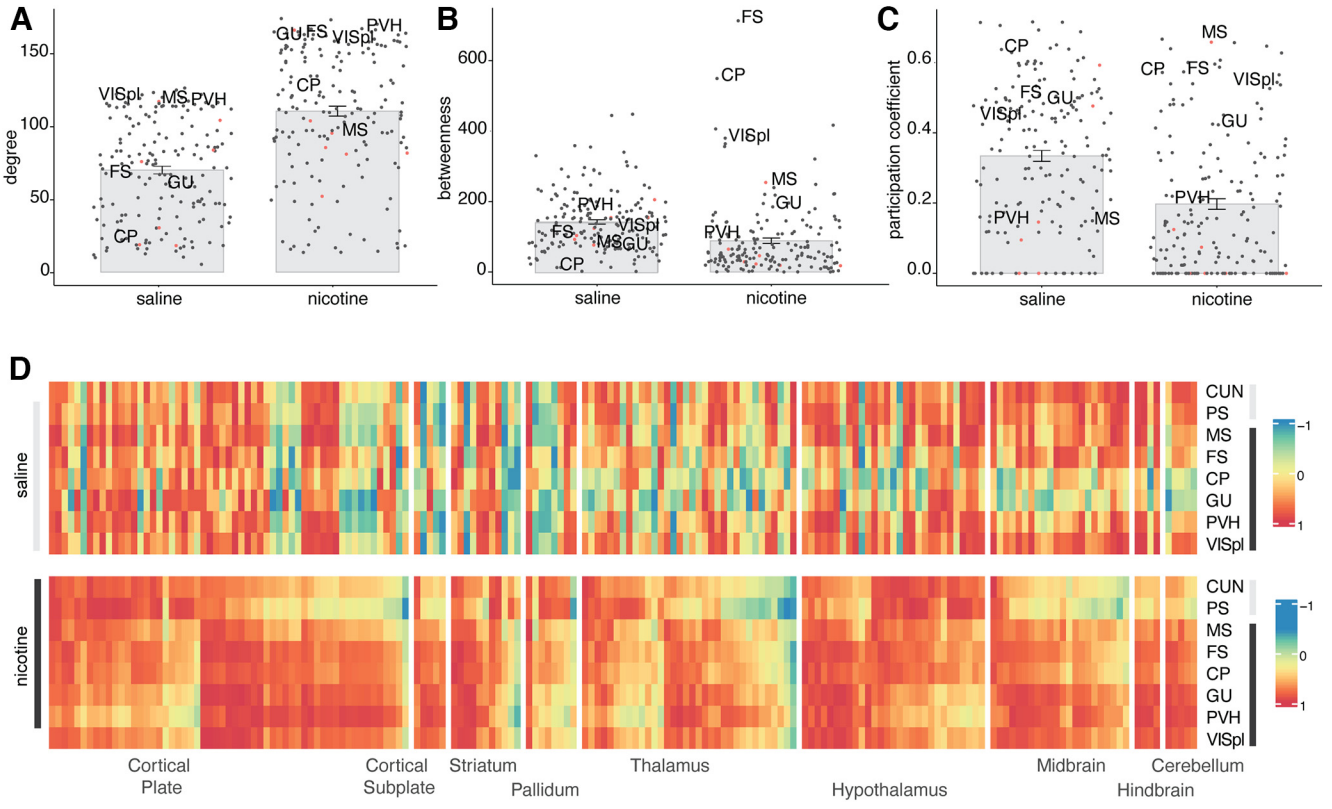

Figure 3 Centrality measurements for hub regions in the saline and nicotine networks. ***A–C***, Degree ($p < 2.2\text{e-}16$[c]; ***A***), betweenness ($p = 2.0\text{e-}08$[d]; ***B***), and participation coefficient ($p = 3.5\text{e-}9$[e]; ***C***), with the long-range cholinergic regions identifiable by a red dot and the hub regions for nicotine withdrawal labeled. ***D***, Heatmap representation of the correlation of the hub regions to all individual regions in the brain (order of the regions same as in Extended Data Fig. 2-1).

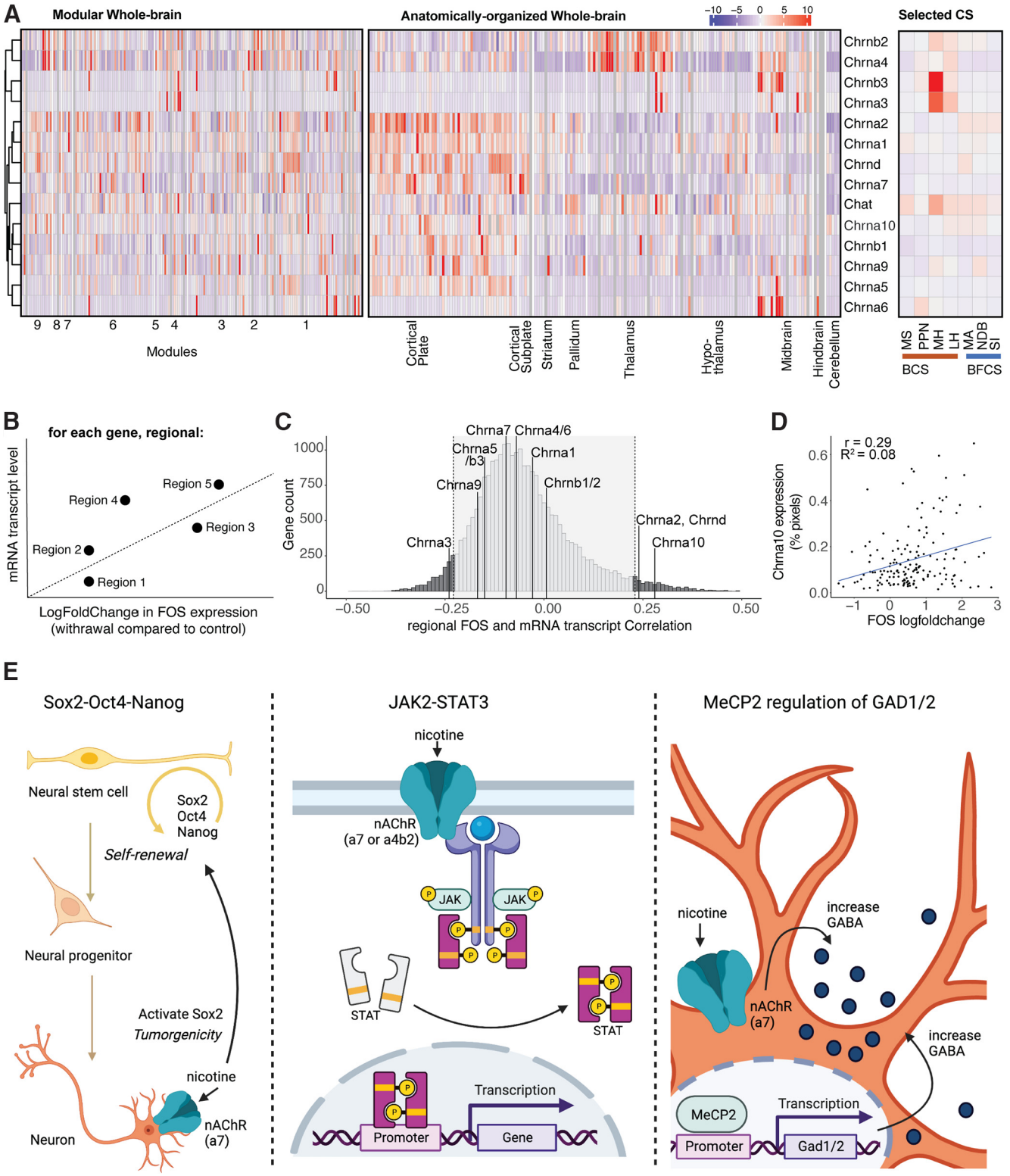

Figure 4. Whole-brain expression distribution of cholinergic receptor subunits, cholinergic transferase, and other proteins. ***A***, Expression density throughout the whole brain hierarchically clustered by row and split into the modules of the nicotine-withdrawal network (left; Fig. 1*C*, ordering of regions; Extended Data Fig. 1-1, list), split into anatomic groups (middle; Fig. 2*E*, ordering of regions; Extended Data Fig. 2-1, list) and the selected long-range cholinergic groups (right; Fig. 2*B*, ordering of the regions). ***B***, Schematic diagram of the correlation analysis for each gene between basal mRNA expression level and nicotine withdrawal-induced Fos transcriptional change in each region. ***C***, Histogram of the number of genes (count) for all found correlations. ***D***, Example correlation graph for the most correlated cholinergic-related gene Chrna10. ***E***, Schematic representations of the pathways identified by

continued
the Reactome analysis for the identified significantly correlated genes: Oct4, Sox2, and Nanog activating genes related to proliferation (left), gene expression by JAK-STAT signaling (middle), and the MeCP2 pathway for regulating the transcription for genes involved in GABA signaling through GAD1 and GAD2 (right), with the potential involvement of nicotine.

($p = 1.08e{-2}$), and methyl CpG binding protein 2 (MeCP2) regulation of transcription of genes involved in GABA signaling ($p = 6.91e{-3}$; Fig. 4*E*).

Discussion

This work follows up on the published established whole-brain nicotine withdrawal network obtained through single-cell whole-brain imaging of the immediate early gene c-Fos compared with controls (Kimbrough et al., 2021), focusing on the long-range cholinergic regions to help interpret and understand specific functional connectome changes. Contrary to our hypothesis, the well defined long-range cholinergic groups (Ch1–7) were not found to cluster together, but rather were distributed throughout the nicotine withdrawal network. Cholinergic regions showed increased functional connectivity with all regions of the brain through two anticorrelated subnetworks separated into basal forebrain-projecting and brainstem-thalamic-projecting cholinergic regions, validating a long-standing hypothesis of the organization of the brain cholinergic systems. Most of the cholinergic-related genes were found to have whole-brain expression profiles that correlated poorly with the nicotine withdrawal-induced Fos changes except for *Chrna2*, *Chrna3*, *Chrna10*, and *Chrnd* mRNA. Finally, we identified a list of >1700 genes for which the baseline expression correlated significantly with the altered brain reactivity in the nicotine withdrawal state and identified cellular pathways that may contribute to neuronal activation during nicotine withdrawal.

This report demonstrates that each of the main modules in the nicotine withdrawal network includes at least one of the well defined long-range cholinergic groups (Ch1–7), and that the localization of each group within each module was consistent with known anatomic and functional connections for these groups (Fig. 1). Cholinergic group 1 is the primary cholinergic input to the hippocampus (Teles-Grilo Ruivo and Mellor, 2013; Müller and Remy, 2018) and was found in the cortico-hypothalamus module. Cholinergic group 5 is the primary cholinergic input for the brainstem (Grofova and Keane, 1991; Mena-Segovia and Bolam, 2017) and was part of the cortico-mid-hindbrain module. Cholinergic groups 2, 3, and 4 are the primary projections to the isocortex, striatum, and amygdala (Mesulam et al., 1983; Luiten et al., 1987; Alheid and Heimer, 1988) and were found in the orbitofrontal-extended amygdalar and cortico-hypothalamic modules. Finally, cholinergic group 7 projects to the brainstem and was found in the midbrain-thalamo-habenular module. Cholinergic neurons have been described to act and project globally rather than modularly, which helps in communication throughout the whole brain (Mesulam et al., 1983; Woolf, 1991).

Nicotine withdrawal had strong effects on the functional connectome. First, the functional connectivity was increased between the long-range cholinergic regions and the rest of the brain (Fig. 2), particularly with the regions that had lower functional connectivity under control conditions such as the cortical plate, striatum, thalamus, and hypothalamus. The increased synchronization between the long-range cholinergic regions and the rest of the brain may contribute to the synchronization of Fos activity throughout the brain, resulting in decreased modularity (Kimbrough et al., 2021). A possible mechanism underlying this brain-wide synchronization is a global increase in acetylcholine release during withdrawal (Rada et al., 2001; Carcoba et al., 2014), leading to the activation of nAChRs, intracellular cation influx, and activation of multiple intracellular cascades activating c-Fos transcription (Merlo Pich et al., 1999; Hu et al., 2002; Changeux, 2010; Mizuno et al., 2015). These results are in line with human fMRI data, where increases in resting-state connectivity during nicotine withdrawal have also been observed (Fedota and Stein, 2015). Moreover, increased local connectivity within specific network nodes correlate with subjective measures of nicotine craving and measures of nicotine dependence (Claus et al., 2013; Janes et al., 2014; Moran-Santa Maria et al., 2015).

Second, nicotine withdrawal caused a functional reorganization of the long-range cholinergic network composed of the MA, NDB, and SI on one side, and the MS, PPN, MH, and LH on the other side, which are correlated within, anticorrelated between, and connected to mostly nonoverlapping regions in the brain. Also, when looking at a minimal network containing the long-range cholinergic regions and key regions known to be involved in addiction, the same findings were illustrated, as follows: (1) increased functional connectivity among the cholinergic groups 2, 3, 4, and 7 and the anterior cingulate, infralimbic, prelimbic, dorsal peduncular, ventral tegmental area, caudoputamen, nucleus accumbens, basolateral and central amygdala, bed nucleus of the stria terminalis, and interpeduncular nucleus; and (2) increased subdivision of the circuitry in basal forebrain and brainstem-thalamic cholinergic systems. Indeed, several cholinergic regions (MH, MA, NDB) were not incorporated in this minimal network under control conditions. The organization of a basal forebrain and a brainstem cholinergic system resembles the original anatomic descriptions of the basal forebrain and brainstem cholinergic systems by Mesulam et al. (1983), Woolf (1991), and George et al. (2006), which not only validates the approach of single-cell whole-brain imaging for functional connectome analysis, but has profound implications from a theoretical point of view. Indeed, it suggests that the different cholinergic regions throughout the brain are not independent from each other, but instead are functionally connected through two opposite systems: a basal forebrain cholinergic system and a brainstem cholinergic system. Nicotine withdrawal then emerges with the dysregulation of these two systems that become anticorrelated. Whether one cholinergic system inhibits the other

or whether they are anticorrelated though the action of a third system remains to be tested.

Third, the central hubs of the network changed. In the saline control network, the CUN and PS acted as hub regions with high degree and betweenness, measures of network centrality (Fig. 3; Wheeler et al., 2013). Following nicotine withdrawal, the fundus of the striatum and caudoputamen were identified as hub regions with the high network centrality measures degree and betweenness. The long-range cholinergic region MS (cholinergic group 1), which is the main input of the hippocampus and has been associated with the anxiogenic effects of nicotine (Zarrindast et al., 2013) had a high participation coefficient and therefore also participated as a hub, especially in the connection between the different modules. Its connector role between the basal forebrain and brainstem cholinergic systems was already illustrated in Figure 2*B*. While the fundus of the striatum is typically not recognized as a long-range cholinergic region, it is a transition zone between the ventral part of the caudoputamen and the substantia innominate (cholinergic group 4) that expresses high levels of acetylcholine esterase and where dopamine release is under a particular tight cholinergic control (O'Connor et al., 1995). The caudoputamen is the brain region with the highest basal acetylcholine level because of a dense cholinergic arborization originating from cholinergic interneurons (Zhou et al., 2002; Gonzales and Smith, 2015; Abudukeyoumu et al., 2019). Caudoputamen cholinergic interneurons are critical to dopamine release, reinforcement learning and the formation of habit (Knowlton et al., 1996; Matsumoto et al., 1999; Kitabatake et al., 2003). These hub regions all play central roles in orchestrating the negative emotional state under nicotine withdrawal and were all found together in the intermediate-size module 3 (Extended Data Figs. 1-1, 1-3). The medial septum—fundus of the striatum—caudoputamen module might thus function as the main nicotine-responsive module that orchestrates the whole-brain response.

All nicotinic receptor genes, except the muscle-type CHRNB1, including eight genomic regions containing 11 neuronal CHRN genes and 3 genomic regions containing 4 muscle-type CHRN genes, have been significantly associated with nicotine dependence and/or alcohol dependence (Zuo et al., 2016). Analysis of the correlation between baseline mRNA expression of the nAChRs in all brain regions with the withdrawal-induced change in Fos expression (Fig. 4*B*) showed significant correlation for *Chrna2*, *Chrna3*, *Chrna10*, and *Chrnd* (Fig. 4*C*,*D*). *Chrna2* has been identified in human genome-wide association studies (GWASs) in association with smoking-related behaviors, like smoking status, smoking initiation, cigarettes smoked per day, and smoking cessation (Liu et al., 2019; Xu et al., 2020). *Chrna3* is part of a locus on chromosome 15q25 with *Chrna5* and *Chrnb4*, which has also been identified in human GWASs to be associated with smoking-related behaviors and nicotine dependence. One single nucleotide polymorphism is specifically localized in *Chrna3* (Spitz et al., 2008; Liu et al., 2010). *Chrna10* was identified through linkage analysis in sibling pairs for nicotine withdrawal (Pergadia et al., 2009) and was found, together with *Chrnd*, to increase the risk for nicotine dependence in an African American population subset (Saccone et al., 2010). It is important to note that these correlations were obtained using baseline gene expression with no exposure to nicotine, suggesting that these genes may be predisposing factors to nicotine dependence. However, further studies are required to examine the correlation between withdrawal-induced gene expression and withdrawal-induced Fos activity. Looking at the mRNA expression was a first attempt to link nAChRs levels to Fos activation. A limitation is that mRNA expression does not necessarily correlate with protein levels or even functional activity of the protein; therefore, while we observed significant correlations between some nAChRs and differential Fos expression, it is possible that negative results for other subunits may be because of a lack of correlation between mRNA levels and protein levels, for instance because of post-transcriptional events (Mousavi et al., 2003).

Other study limitations are associated with the dataset. Fos is inherently not a great marker for neuronal inhibition and therefore poorly detects negative correlations between brain regions resulting from activation of inhibitory neurons. The use of the recently identified marker for neuronal inhibition could reduce this gap in future studies (Yang et al., 2023). The dataset also has a relatively low sample size. In our experience, the comparison of groups of brain regions that are correlated versus regions that are not correlated (among the $\geq$175 brain regions) is associated with large effect sizes (Cohen *d*, $>$1.8) and requires only $N = 4$–5/group for significant findings, which is in line with what has been reported previously (Wheeler et al., 2013; Orsini et al., 2018; Kimbrough et al., 2020, 2021). A higher sample size would increase the ability to detect effects that have moderate to small size and further dissect the different brain networks contributing to nicotine dependence. Finally, both the original whole-brain reactivity (Kimbrough et al., 2021) and whole-brain gene expression (Lein et al., 2007) studies only incorporated male subjects in their study and database precluding any analysis of sex differences. Follow-up studies are needed to evaluate whether these effects also exist in females.

We then extended the gene analysis to include the mRNA transcript levels of all 19,413 genes of the *in situ* hybridization gene expression Allen Brain Atlas database, which resulted in a list of 1755 genes that had significant correlations between their expression and the nicotine withdrawal-induced Fos changes. Through pathway analysis (Joshi-Tope et al., 2005), we identified potentially promising genes and pathways that may contribute to the Fos expression during nicotine withdrawal. The first pathway contained the transcription factors *Sox2*, *Oct4*, and *Nanog*, which are highly expressed in proliferative adult neurogenesis precursor cells in discrete brain regions (Suh et al., 2007; Bennett et al., 2009; Ahlfeld et al., 2017; Stevanovic et al., 2021) that are associated with Fos expression (Velazquez et al., 2015) and have been reported to be affected by nicotine (Brooks and Henderson, 2021). The second pathway was part of the immune response by JAK2-STAT3, which has been shown to be activated by nicotine through complex formation with Chrna7 or Crna4/

Chrnab2 to provide neuroprotective effects (Shaw et al., 2002; Wang et al., 2022). The third pathway brings up another very relevant transcription factor, MeCP2, which is mutated in the neurodevelopmental disorder Rett syndrome (Amir et al., 1999). MeCP2 knock-out mice have reduced ChAT-positive cells, which reduced Chrna4 and Chrna6 expression, an attenuated behavior response to nicotine (Leung et al., 2017), dysfunctional reduced GABA signaling (Chao et al., 2010), and some reversed deficits following nicotine administration (Zhang et al., 2016). MeCP2 has been shown to modulate the effects of drugs of abuse in preclinical models (Deng et al., 2010; Im et al., 2010; Repunte-Canonigo et al., 2014; Xu et al., 2021). GABA signaling, regulated by MeCP2 through GAD1 and GAD2 that were both in the gene list, has a well established role in nicotine dependence and withdrawal (Markou, 2008; D'Souza and Markou, 2013; Klenowski et al., 2022). Despite relatively low significance for these pathways (loss of significance with correction for multiple comparisons; false discovery rate, 80%), the top three identified pathways have been shown to be affected by or associated with nicotine, providing validity to this exploratory approach, which might be a way to further process and investigate the obtained whole-brain functional connectome datasets. Finally, these results demonstrate the power of using single-cell whole-brain imaging combined with whole-brain transcriptomics to identify new brain regions, new gene targets, and new cellular pathways that may contribute to nicotine dependence and substance use disorder in general.

In conclusion, these results demonstrate that cholinergic regions increased functional connectivity with the rest of the brain through two anticorrelated subnetworks separated into basal forebrain projecting and brainstem-thalamic-projecting cholinergic regions. The expression level of *Chrna2*, *Chrna3*, *Chrna10*, and *Chrnd* mRNA throughout the brain was correlated with the nicotine withdrawal-induced Fos changes. Finally, we have identified a list of over ~1700 genes for which the baseline expression correlates significantly with the altered brain reactivity in the nicotine withdrawal state and identified cellular pathways that may contribute to neuronal activation during nicotine withdrawal.

References

Abudukeyoumu N, Hernandez-Flores T, Garcia-Munoz M, Arbuthnott GW (2019) Cholinergic modulation of striatal microcircuits. Eur J Neurosci 49:604–622.

Abulseoud OA, Ross TJ, Nam HW, Caparelli EC, Tennekoon M, Schleyer B, Castillo J, Fedota J, Gu H, Yang Y, Stein E (2020) Short-term nicotine deprivation alters dorsal anterior cingulate glutamate concentration and concomitant cingulate-cortical functional connectivity. Neuropsychopharmacology 45:1920–1930.

Ahlfeld J, Filser S, Schmidt F, Wefers AK, Merk DJ, Glass R, Herms J, Schüller U (2017) Neurogenesis from Sox2 expressing cells in the adult cerebellar cortex. Sci Rep 7:6137.

Aishah A, Hinton T, Machaalani R (2017) Cellular protein and mRNA expression of β1 nicotinic acetylcholine receptor (nAChR) subunit in brain, skeletal muscle and placenta. Int J Dev Neurosci 58:9–16.

Alheid GF, Heimer L (1988) New perspectives in basal forebrain organization of special relevance for neuropsychiatric disorders: the striatopallidal, amygdaloid, and corticopetal components of substantia innominata. Neuroscience 27:1–39.

Allen SS, Bade T, Hatsukami D, Center B (2008) Craving, withdrawal, and smoking urges on days immediately prior to smoking relapse. Nicotine Tob Res 10:35–45.

Amir RE, Van den Veyver IB, Wan M, Tran CQ, Francke U, Zoghbi HY (1999) Rett syndrome is caused by mutations in X-linked MECP2, encoding methyl-CpG-binding protein 2. Nat Genet 23:185–188.

Baiamonte BA, Valenza M, Roltsch EA, Whitaker AM, Baynes BB, Sabino V, Gilpin NW (2014) Nicotine dependence produces hyperalgesia: role of corticotropin-releasing factor-1 receptors (CRF1Rs) in the central amygdala (CeA). Neuropharmacology 77:217–223.

Balfour DJ, Fagerström KO (1996) Pharmacology of nicotine and its therapeutic use in smoking cessation and neurodegenerative disorders. Pharmacol Ther 72:51–81.

Bennett L, Yang M, Enikolopov G, Iacovitti L (2009) Circumventricular organs: a novel site of neural stem cells in the adult brain. Mol Cell Neurosci 41:337–347.

Benwell ME, Balfour DJ, Anderson JM (1988) Evidence that tobacco smoking increases the density of (-)-[3H]nicotine binding sites in human brain. J Neurochem 50:1243–1247.

Bergstrom HC, Smith RF, Mollinedo NS, McDonald CG (2010) Chronic nicotine exposure produces lateralized, age-dependent dendritic remodeling in the rodent basolateral amygdala. Synapse 64:754–764.

Brooks AC, Henderson BJ (2021) Systematic review of nicotine exposure's effects on neural stem and progenitor cells. Brain Sci 11:172.

Brown R (2006) What is a brain state? Phil Psychol 19:729–742.

Carcoba LM, Orfila JE, Natividad LA, Torres OV, Pipkin JA, Ferree PL, Castañeda E, Moss DE, O'Dell LE (2014) Cholinergic transmission during nicotine withdrawal is influenced by age and pre-exposure to nicotine: implications for teenage smoking. Dev Neurosci 36:347–355.

Changeux JP (2010) Nicotine addiction and nicotinic receptors: lessons from genetically modified mice. Nat Rev Neurosci 11:389–401.

Chao HT, Chen H, Samaco RC, Xue M, Chahrour M, Yoo J, Neul JL, Gong S, Lu HC, Heintz N, Ekker M, Rubenstein JL, Noebels JL, Rosenmund C, Zoghbi HY (2010) Dysfunction in GABA signalling mediates autism-like stereotypies and Rett syndrome phenotypes. Nature 468:263–269.

Cheng W, Rolls ET, Robbins TW, Gong W, Liu Z, Lv W, Du J, Wen H, Ma L, Quinlan EB, Garavan H, Artiges E, Papadopoulos Orfanos D, Smolka MN, Schumann G, Kendrick K, Feng J (2019) Decreased brain connectivity in smoking contrasts with increased connectivity in drinking. eLife 8:e40765.

Claus ED, Blaine SK, Filbey FM, Mayer AR, Hutchison KE (2013) Association between nicotine dependence severity, BOLD response to smoking cues, and functional connectivity. Neuropsychopharmacology 38:2363–2372.

D'Souza MS, Markou A (2013) The "stop" and "go" of nicotine dependence: role of GABA and glutamate. Cold Spring Harb Perspect Med 3:a012146.

Dani JA, Heinemann S (1996) Molecular and cellular aspects of nicotine abuse. Neuron 16:905–908.

Davoudian PA, Shao L-X, Kwan AC (2023) Shared and distinct brain regions targeted for immediate early gene expression by ketamine and psilocybin. ACS Chem Neurosci 14:468–480.

Deng JV, Rodriguiz RM, Hutchinson AN, Kim IH, Wetsel WC, West AE (2010) MeCP2 in the nucleus accumbens contributes to neural and behavioral responses to psychostimulants. Nat Neurosci 13:1128–1136.

Fedota JR, Stein EA (2015) Resting-state functional connectivity and nicotine addiction: prospects for biomarker development. Ann N Y Acad Sci 1349:64–82.

Fowler CD, Turner JR, Imad DM (2020) Molecular mechanisms associated with nicotine pharmacology and dependence. Handb Exp Pharmacol 258:373–393.

Fulcher BD, Fornito A (2016) A transcriptional signature of hub connectivity in the mouse connectome. Proc Natl Acad Sci U S A 113:1435–1440.
Fulcher BD, Murray JD, Zerbi V, Wang X-J (2019) Multimodal gradients across mouse cortex. Proc Natl Acad Sci U S A 116:4689–4695.
Funk D, Coen K, Tamadon S, Hope BT, Shaham Y, Lê AD (2016) Role of central amygdala neuronal ensembles in incubation of nicotine craving. J Neurosci 36:8612–8623.
George O, Koob GF (2010) Individual differences in prefrontal cortex function and the transition from drug use to drug dependence. Neurosci Biobehav Rev 35:232–247.
George O, Vallée M, Le Moal M, Mayo W (2006) Neurosteroids and cholinergic systems: implications for sleep and cognitive processes and potential role of age-related changes. Psychopharmacology (Berl) 186:402–413.
Gil SM, Metherate R (2019) Enhanced sensory-cognitive processing by activation of nicotinic acetylcholine receptors. Nicotine Tob Res 21:377–382.
Gonzales KK, Smith Y (2015) Cholinergic interneurons in the dorsal and ventral striatum: anatomical and functional considerations in normal and diseased conditions. Ann N Y Acad Sci 1349:1–45.
Govind AP, Vezina P, Green WN (2009) Nicotine-induced upregulation of nicotinic receptors: underlying mechanisms and relevance to nicotine addiction. Biochem Pharmacol 78:756–765.
Grieder TE, et al. (2014) VTA CRF neurons mediate the aversive effects of nicotine withdrawal and promote intake escalation. Nat Neurosci 17:1751–1758.
Grofova I, Keane S (1991) Descending brainstem projections of the pedunculopontine tegmental nucleus in the rat. Anat Embryol (Berl) 184:275–290.
Hahn B (2015) Nicotinic receptors and attention. Curr Top Behav Neurosci 23:103–135.
Hobkirk AL, Nichols TT, Foulds J, Yingst JM, Veldheer S, Hrabovsky S, Richie J, Eissenberg T, Wilson SJ (2018) Changes in resting state functional brain connectivity and withdrawal symptoms are associated with acute electronic cigarette use. Brain Res Bull 138:56–63.
Hong LE, Gu H, Yang Y, Ross TJ, Salmeron BJ, Buchholz B, Thaker GK, Stein EA (2009) Association of nicotine addiction and nicotine's actions with separate cingulate cortex functional circuits. Arch Gen Psychiatry 66:431–441.
Hu M, Liu QS, Chang KT, Berg DK (2002) Nicotinic regulation of CREB activation in hippocampal neurons by glutamatergic and nonglutamatergic pathways. Mol Cell Neurosci 21:616–625.
Huang W, Tam K, Fernando J, Heffernan M, King J, DiFranza JR (2015) Nicotine and resting-state functional connectivity: effects of intermittent doses. Nicotine Tob Res 17:1311–1317.
Im HI, Hollander JA, Bali P, Kenny PJ (2010) MeCP2 controls BDNF expression and cocaine intake through homeostatic interactions with microRNA-212. Nat Neurosci 13:1120–1127.
Janes AC, Farmer S, Frederick B, Nickerson LD, Lukas SE (2014) An increase in tobacco craving is associated with enhanced medial prefrontal cortex network coupling. PLoS One 9:e88228.
Johnson PM, Hollander JA, Kenny PJ (2008) Decreased brain reward function during nicotine withdrawal in C57BL6 mice: evidence from intracranial self-stimulation (ICSS) studies. Pharmacol Biochem Behav 90:409–415.
Joshi-Tope G, Gillespie M, Vastrik I, D'Eustachio P, Schmidt E, de Bono B, Jassal B, Gopinath GR, Wu GR, Matthews L, Lewis S, Birney E, Stein L (2005) Reactome: a knowledgebase of biological pathways. Nucleic Acids Res 33:D428–D432.
Kimbrough A, Lurie DJ, Collazo A, Kreifeldt M, Sidhu H, Macedo GC, D'Esposito M, Contet C, George O (2020) Brain-wide functional architecture remodeling by alcohol dependence and abstinence. Proc Natl Acad Sci U S A 117:2149–2159.
Kimbrough A, Kallupi M, Smith LC, Simpson S, Collazo A, George O (2021) Characterization of the brain functional architecture of psychostimulant withdrawal using single-cell whole-brain imaging. eNeuro 8:ENEURO.0208-19.2021.
Kitabatake Y, Hikida T, Watanabe D, Pastan I, Nakanishi S (2003) Impairment of reward-related learning by cholinergic cell ablation in the striatum. Proc Natl Acad Sci U S A 100:7965–7970.
Klenowski PM, Zhao-Shea R, Freels TG, Molas S, Tapper AR (2022) Dynamic activity of interpeduncular nucleus GABAergic neurons controls expression of nicotine withdrawal in male mice. Neuropsychopharmacology 47:641–651.
Knowlton BJ, Mangels JA, Squire LR (1996) A neostriatal habit learning system in humans. Science 273:1399–1402.
Kutlu MG, Tumolo JM, Holliday E, Garrett B, Gould TJ (2016) Acute nicotine enhances spontaneous recovery of contextual fear and changes c-fos early gene expression in infralimbic cortex, hippocampus, and amygdala. Learn Mem 23:405–414.
Le Foll B, Goldberg SR (2009) Effects of nicotine in experimental animals and humans: an update on addictive properties. Handb Exp Pharmacol (192):335–367.
Lein ES, et al. (2007) Genome-wide atlas of gene expression in the adult mouse brain. Nature 445:168–176.
Leslie FM, Mojica CY, Reynaga DD (2013) Nicotinic receptors in addiction pathways. Mol Pharmacol 83:753–758.
Leung J, McPhee DM, Renda A, Penty N, Farhoomand F, Nashmi R, Delaney KR (2017) MeCP2-deficient mice have reduced α4 and α6 nicotinic receptor mRNA and altered behavioral response to nicotinic agonists. Behav Brain Res 330:118–126.
Liu JZ, et al (2010) Meta-analysis and imputation refines the association of 15q25 with smoking quantity. Nat Genet 42:436–440.
Liu M, et al (2019) Association studies of up to 1.2 million individuals yield new insights into the genetic etiology of tobacco and alcohol use. Nat Genet 51:237–244.
Luiten PG, Gaykema RP, Traber J, Spencer DG Jr (1987) Cortical projection patterns of magnocellular basal nucleus subdivisions as revealed by anterogradely transported Phaseolus vulgaris leucoagglutinin. Brain Res 413:229–250.
Markou A (2008) Review. Neurobiology of nicotine dependence. Philos Trans R Soc Lond B Biol Sci 363:3159–3168.
Martin-Soelch C (2013) Neuroadaptive changes associated with smoking: structural and functional neural changes in nicotine dependence. Brain Sci 3:159–176.
Matsumoto N, Hanakawa T, Maki S, Graybiel AM, Kimura M (1999) Role of nigrostriatal dopamine system in learning to perform sequential motor tasks in a predictive manner. J Neurophysiol 82:978–998.
Mena-Segovia J, Bolam JP (2017) Rethinking the pedunculopontine nucleus: from cellular organization to function. Neuron 94:7–18.
Merlo Pich E, Chiamulera C, Carboni L (1999) Molecular mechanisms of the positive reinforcing effect of nicotine. Behav Pharmacol 10:587–596.
Mesulam MM, Mufson EJ, Levey AI, Wainer BH (1983) Cholinergic innervation of cortex by the basal forebrain: cytochemistry and cortical connections of the septal area, diagonal band nuclei, nucleus basalis (substantia innominata), and hypothalamus in the rhesus monkey. J Comp Neurol 214:170–197.
Mizuno K, Kurokawa K, Ohkuma S (2015) Nicotinic acetylcholine receptors regulate type 1 inositol 1,4,5-trisphosphate receptor expression via calmodulin kinase IV activation. J Neurosci Res 93:660–665.
Molas S, DeGroot SR, Zhao-Shea R, Tapper AR (2017) Anxiety and nicotine dependence: emerging role of the habenulo-interpeduncular axis. Trends Pharmacol Sci 38:169–180.
Moran-Santa Maria MM, Hartwell KJ, Hanlon CA, Canterberry M, Lematty T, Owens M, Brady KT, George MS (2015) Right anterior insula connectivity is important for cue-induced craving in nicotine-dependent smokers. Addict Biol 20:407–414.
Mousavi M, Hellström-Lindahl E, Guan Z-Z, Shan K-R, Ravid R, Nordberg A (2003) Protein and mRNA levels of nicotinic receptors in brain of tobacco using controls and patients with Alzheimer's disease. Neuroscience 122:515–520.
Müller C, Remy S (2018) Septo-hippocampal interaction. Cell Tissue Res 373:565–575.

Muskens JB, Schellekens AFA, de Leeuw FE, Tendolkar I, Hepark S (2012) Damage in the dorsal striatum alleviates addictive behavior. Gen Hosp Psychiatry 34:702.e709–702.e711.

O'Connor WT, Drew KL, Ungerstedt U (1995) Differential cholinergic regulation of dopamine release in the dorsal and ventral neostriatum of the rat: an *in vivo* microdialysis study. J Neurosci 15:8353–8361.

Orsini CA, Colon-Perez LM, Heshmati SC, Setlow B, Febo M (2018) Functional connectivity of chronic cocaine use reveals progressive neuroadaptations in neocortical, striatal, and limbic networks. eNeuro 5:ENEURO.0081-18.2018.

Pang X, Liu L, Ngolab J, Zhao-Shea R, McIntosh JM, Gardner PD, Tapper AR (2016) Habenula cholinergic neurons regulate anxiety during nicotine withdrawal via nicotinic acetylcholine receptors. Neuropharmacology 107:294–304.

Pergadia ML, Agrawal A, Loukola A, Montgomery GW, Broms U, Saccone SF, Wang JC, Todorov AA, Heikkilä K, Statham DJ, Henders AK, Campbell MJ, Rice JP, Todd RD, Heath AC, Goate AM, Peltonen L, Kaprio J, Martin NG, Madden PAF (2009) Genetic linkage findings for DSM-IV nicotine withdrawal in two populations. Am J Med Genet B Neuropsychiatr Genet 150B:950–959.

Qi X, Guzhva L, Yang Z, Febo M, Shan Z, Wang KKW, Bruijnzeel AW (2016) Overexpression of CRF in the BNST diminishes dysphoria but not anxiety-like behavior in nicotine withdrawing rats. Eur Neuropsychopharmacol 26:1378–1389.

Rada P, Jensen K, Hoebel BG (2001) Effects of nicotine and mecamylamine-induced withdrawal on extracellular dopamine and acetylcholine in the rat nucleus accumbens. Psychopharmacology (Berl) 157:105–110.

Reisiger A-R, Kaufling J, Manzoni O, Cador M, Georges F, Caillé S (2014) Nicotine self-administration induces CB1-dependent LTP in the bed nucleus of the stria terminalis. J Neurosci 34:4285–4292.

Renier N, Wu Z, Simon DJ, Yang J, Ariel P, Tessier-Lavigne M (2014) iDISCO: a simple, rapid method to immunolabel large tissue samples for volume imaging. Cell 159:896–910.

Renier N, Adams EL, Kirst C, Wu Z, Azevedo R, Kohl J, Autry AE, Kadiri L, Umadevi Venkataraju K, Zhou Y, Wang VX, Tang CY, Olsen O, Dulac C, Osten P, Tessier-Lavigne M (2016) Mapping of brain activity by automated volume analysis of immediate early genes. Cell 165:1789–1802.

Repunte-Canonigo V, Chen J, Lefebvre C, Kawamura T, Kreifeldt M, Basson O, Roberts AJ, Sanna PP (2014) MeCP2 regulates ethanol sensitivity and intake. Addict Biol 19:791–799.

Roland AV, Coelho CAO, Haun HL, Gianessi CA, Lopez MF, D'Ambrosio S, Machinski SN, Kroenke CD, Frankland PW, Becker HC, Kash TL (2022) Alcohol dependence modifies brain networks activated during abstinence and reaccess: a c-fos-based analysis in mice. bioRxiv. Advance online publication. Retrieved June 10, 2023. doi:.

Rubinov M, Sporns O (2010) Complex network measures of brain connectivity: uses and interpretations. Neuroimage 52:1059–1069.

Saccone NL, Schwantes-An TH, Wang JC, Grucza RA, Breslau N, Hatsukami D, Johnson EO, Rice JP, Goate AM, Bierut LJ (2010) Multiple cholinergic nicotinic receptor genes affect nicotine dependence risk in African and European Americans. Genes Brain Behav 9:741–750.

Schmidt BL, Tambeli CH, Gear RW, Levine JD (2001) Nicotine withdrawal hyperalgesia and opioid-mediated analgesia depend on nicotine receptors in nucleus accumbens. Neuroscience 106:129–136.

Semenova S, Jin X, McClure-Begley TD, Tadman MP, Marks MJ, Markou A (2018) Differential effects of withdrawal from intermittent and continuous nicotine exposure on reward deficit and somatic aspects of nicotine withdrawal and expression of $\alpha4\beta2^*$ nAChRs in Wistar male rats. Pharmacol Biochem Behav 171:54–65.

Sharp BM (2019) Basolateral amygdala, nicotinic cholinergic receptors, and nicotine: pharmacological effects and addiction in animal models and humans. Eur J Neurosci 50:2247–2254.

Shaw S, Bencherif M, Marrero MB (2002) Janus kinase 2, an early target of alpha 7 nicotinic acetylcholine receptor-mediated neuroprotection against Abeta-(1-42) amyloid. J Biol Chem 277:44920–44924.

Simmons SJ, Gentile TA, Mo L, Tran FH, Ma S, Muschamp JW (2016) Nicotinic receptor blockade decreases fos immunoreactivity within orexin/hypocretin-expressing neurons of nicotine-exposed rats. Behav Brain Res 314:226–233.

Smith ACW, Jonkman S, Difeliceantonio AG, O'Connor RM, Ghoshal S, Romano MF, Everitt BJ, Kenny PJ (2021) Opposing roles for striatonigral and striatopallidal neurons in dorsolateral striatum in consolidating new instrumental actions. Nat Commun 12:5121.

Spitz MR, Amos CI, Dong Q, Lin J, Wu X (2008) The CHRNA5-A3 region on chromosome 15q24-25.1 is a risk factor both for nicotine dependence and for lung cancer. J Natl Cancer Inst 100:1552–1556.

Stevanovic M, Drakulic D, Lazic A, Ninkovic DS, Schwirtlich M, Mojsin M (2021) SOX Transcription factors as important regulators of neuronal and glial differentiation during nervous system development and adult neurogenesis. Front Mol Neurosci 14:654031.

Stoker AK, Olivier B, Markou A (2012) Involvement of metabotropic glutamate receptor 5 in brain reward deficits associated with cocaine and nicotine withdrawal and somatic signs of nicotine withdrawal. Psychopharmacology (Berl) 221:317–327.

Suh H, Consiglio A, Ray J, Sawai T, D'Amour KA, Gage FH (2007) In vivo fate analysis reveals the multipotent and self-renewal capacities of Sox2+ neural stem cells in the adult hippocampus. Cell Stem Cell 1:515–528.

Teles-Grilo Ruivo LM, Mellor JR (2013) Cholinergic modulation of hippocampal network function. Front Synaptic Neurosci 5:2.

Ueda HR, Dodt HU, Osten P, Economo MN, Chandrashekar J, Keller PJ (2020) Whole-brain profiling of cells and circuits in mammals by tissue clearing and light-sheet microscopy. Neuron 106:369–387.

Velazquez FN, Caputto BL, Boussin FD (2015) c-Fos importance for brain development. Aging (Albany NY) 7:1028–1029.

Vetere G, Kenney JW, Tran LM, Xia F, Steadman PE, Parkinson J, Josselyn SA, Frankland PW (2017) Chemogenetic interrogation of a brain-wide fear memory network in mice. Neuron 94:363–374.4.

Wang Q, Gou J, Guo S, Wei F, Han T, Lai R, Zhang D, Diao Y, Yin Y (2022) Nicotine activating $\alpha4\beta2$ nicotinic acetylcholine receptors to suppress neuroinflammation via JAK2-STAT3 signaling pathway in ischemic rats and inflammatory cells. Mol Neurobiol 59:3280–3293.

Wang R, Yi J, Shang J, Yu W, Li Z, Huang H, Xie H, Wang S (2019) 6-Hydroxypseudooxynicotine dehydrogenase delivers electrons to electron transfer flavoprotein during nicotine degradation by *Agrobacterium tumefaciens* S33. Appl Environ Microbiol 85: e00454-19.

Wheeler AL, Teixeira CM, Wang AH, Xiong X, Kovacevic N, Lerch JP, McIntosh AR, Parkinson J, Frankland PW (2013) Identification of a functional connectome for long-term fear memory in mice. PLoS Comput Biol 9:e1002853.

Wills L, Kenny PJ (2021) Addiction-related neuroadaptations following chronic nicotine exposure. J Neurochem 157:1652–1673.

Woolf NJ (1991) Cholinergic systems in mammalian brain and spinal cord. Prog Neurobiol 37:475–524.

Xu K, Li B, McGinnis KA, Vickers-Smith R, Dao C, Sun N, Kember RL, Zhou H, Becker WC, Gelernter J, Kranzler HR, Zhao H, Justice AC (2020) Genome-wide association study of smoking trajectory and meta-analysis of smoking status in 842,000 individuals. Nat Commun 11:5302.

Xu W, Hong Q, Lin Z, Ma H, Chen W, Zhuang D, Zhu H, Lai M, Fu D, Zhou W, Liu H (2021) Role of nucleus accumbens microRNA-181a and MeCP2 in incubation of heroin craving in male rats. Psychopharmacology (Berl) 238:2313–2324.

Yang D, Wang Y, Qi T, Zhang X, Shen L, Ma J, Pang Z, Lal NK, McClatchy DB, Wang K, Xie Y, Polli F, Maximov A, Augustine V,

Cline HT, Yates JR, Ye L (2023) Phosphorylation of pyruvate dehydrogenase marks the inhibition of “in vivo” neuronal activity. bioRxiv. Advance online publication. Retrieved June 10, 2023. doi:.

Zarrindast MR, Tajik R, Ebrahimi-Ghiri M, Nasehi M, Rezayof A (2013) Role of the medial septum cholinoceptors in anxiogenic-like effects of nicotine. Physiol Behav 119:103–109.

Zhang Y, Cao SX, Sun P, He HY, Yang CH, Chen XJ, Shen CJ, Wang XD, Chen Z, Berg DK, Duan S, Li XM (2016) Loss of MeCP2 in cholinergic neurons causes part of RTT-like phenotypes via α7 receptor in hippocampus. Cell Res 26:728–742.

Zhou FM, Wilson CJ, Dani JA (2002) Cholinergic interneuron characteristics and nicotinic properties in the striatum. J Neurobiol 53:590–605.

Zhou X, Nonnemaker J, Sherrill B, Gilsenan AW, Coste F, West R (2009) Attempts to quit smoking and relapse: factors associated with success or failure from the ATTEMPT cohort study. Addict Behav 34:365–373.

Zuo L, Tan Y, Li CR, Wang Z, Wang K, Zhang X, Lin X, Chen X, Zhong C, Wang X, Wang J, Lu L, Luo X (2016) Associations of rare nicotinic cholinergic receptor gene variants to nicotine and alcohol dependence. Am J Med Genet B Neuropsychiatr Genet 171:1057–1071.